

Article

Optimization of Two-Stage IPD-(1+I) Controllers for Frequency Regulation of Sustainable Energy Based Hybrid Microgrid Network

Abdul Latif ¹, S. M. Suhail Hussain ^{2,*} , Dulal Chandra Das ¹  and Taha Selim Ustun ² 

¹ Department of Electrical Engineering, National Institute of Technology Silchar, Assam 788010, India; abdul_rs@ee.nits.ac.in (A.L.); dulal@ee.nits.ac.in (D.C.D.)

² Fukushima Renewable Energy Institute, AIST (FREA), National Institute of Advanced Industrial Science and Technology (AIST), Koriyama 963-0298, Japan; selim.ustun@aist.go.jp

* Correspondence: suhail.hussain@aist.go.jp; Tel.: +91-9957299427

Abstract: Sustainable energy based hybrid microgrids are advantageous in meeting constantly increasing energy demands. Conversely, the intermittent nature of renewable sources represents the main challenge to achieving a reliable supply. Hence, load frequency regulation by adjusting the amount of power shared between subsystems is considered as a promising research field. Therefore, this paper presents a new stratagem for frequency regulation by developing a novel two stage integral-proportional-derivative with one plus integral (IPD-(1+I)) controller for multi sources islanded microgrid system (MS-I μ GS). The proposed stratagem has been tested in an MS-I μ GS comprising of a wind turbine, parabolic trough, biodiesel generators, solid-oxide fuel cell, and electric water heater. The proposed model under different scenarios is simulated in MATLAB environment considering the real-time recorded wind data. A recently developed sine-cosine algorithmic technique (SCA) has been leveraged for optimal regulation of frequency in the considered microgrid. To identify the supremacy of the proposed technique, comparative studies with other classical controllers with different optimization techniques have been performed. From the comparison, it is clearly evident that, SCA-(IPD-(1+I)) controller gives better performance over other considered stratagems in terms of various time domain specific parameters, such as peak deviations (overshoot, undershoot) and settling time. Finally, the robustness of the proposed stratagem is evaluated by conducting sensitivity analysis under $\pm 30\%$ parametric variations and $+30\%$ load demand. The lab tests results validate the operation of the proposed system and show that it can be used to regulate the frequency in stand-alone microgrids with a high penetration of renewable energy.



check for updates

Citation: Latif, A.; Hussain, S.M.S.; Das, D.C.; Ustun, T.S. Optimization of Two-Stage IPD-(1+I) Controllers for Frequency Regulation of Sustainable Energy Based Hybrid Microgrid Network. *Electronics* **2021**, *10*, 919. <https://doi.org/10.3390/electronics10080919>

Academic Editor: Valeri Mladenov

Received: 9 March 2021

Accepted: 8 April 2021

Published: 12 April 2021

Publisher's Note: MDPI stays neutral with regard to jurisdictional claims in published maps and institutional affiliations.



Copyright: © 2021 by the authors. Licensee MDPI, Basel, Switzerland. This article is an open access article distributed under the terms and conditions of the Creative Commons Attribution (CC BY) license (<https://creativecommons.org/licenses/by/4.0/>).

Keywords: two stage integral-proportional-derivative with one plus integral (IPD-(1+I)) controller; frequency regulation; multi sources islanded microgrid system (MS-I μ GS); sine-cosine algorithmic technique

1. Introduction

Modern energy policies require power generation solutions with minimal environmental impact and carbon footprint. The interest in renewable units (RUs) has increased due to the depletion of fossil sources to fulfill the energy demand and use of promising strategic policies [1]. A report of the United Nations shows that around 840 billion people worldwide did not have access to electricity as of 2017 [2]. Most of these people are from remote areas where the accessibility of a centralized conventional grid is very expensive and infeasible. In this circumstance, an islanded microgrid system integrated with RUs is believed to be a cost-effective solution due to the small scale, energy security, and on-site distributed energy which helps to provide a sustainable carbon neutral electrified society. A higher penetration of RUs has led to the widespread renewable microgrid concept achieved through installation of wind, solar PV, solar thermal, bio-generation etc. [3]. The proposed

work considered hybrid microgrid system where two different renewable units such as wind and parabolic solar thermal system are considered. The parabolic-trough solar thermal system is one of the developed and proven solar thermal technologies with significant potential to contribute in energy sector [4]. Moreover, wind and solar energy entirely bank on weather conditions and geographical location. However, these two sources are complementary in nature. In addition, these two renewable sources are the most matured and rapidly developing non-conventional energy resources with an average wind growth of 21% during the last few years. Therefore, the higher penetration of RUs with variable consumer demands causes surplus deviation in the system frequency [5,6]. In fact, the mismatch between total generation and demand may be frequently encountered in hybrid microgrid system which leads to power and frequency fluctuation. To avoid this problem, eco-friendly, non-toxic (low unexhausted hydrocarbon and CO particles) based bio-diesel power generation (BPG) units and lower polluted gas with a higher efficiency based solid-oxide fuel cell (SOFC) could be a possible solution which needs to be explored. BPG has great dynamic response to keep following the load demand and minimizing the frequency fluctuation. Thus, BPG can play a crucial role to maintain the power of an isolated system. To maintain the dynamic responses of frequency, a controllable electric water heater (CEWH) can play a vital role by consuming surplus energy in under-loaded condition. The dynamic performance of CEWH needs to be explored in the proposed multi-sources hybrid microgrid system (MS-I μ GS). Focusing on the above aspect, proper control systems and disturbance mitigation techniques are essential for enhancing future RESs-based power systems [7]. A robust coordinated power management for micro grid power system has been developed in [8]. The authors in [9] developed a distributed novel control strategy for a hybrid micro grid power system where a wide-system control mechanism has been developed for independent control of micro grid. A wide employment of diversified storage units (SUs), such as batteries, flywheels, and ultra-capacitors (UCs), has been leveraged to smoothen the system performance as well as to reduce the pressure on the diesel units [10].

To conserve desired performance during sudden disturbances, a collection of different controllers and algorithmic techniques has been introduced by many researchers in the past [11]. A majority of the studies used traditional proportional-integral (PI) and traditional proportional-integral-derivative (PID) controllers for frequency regulation in renewable microgrids. Authors in [12] targeted load frequency regulation assignment has been analyzed by PI/PID controllers based on genetic algorithm (GA). The authors in [13] have depicted a very commonly used PI controller based on differential evolution (DE) technique. Application of cascaded proportional-integral with proportional derivative (PI-PD) controller based flower pollination optimization (FPO) for frequency response model of microgrid system has been discussed in [14]. The authors have utilized the same FPO technique to optimally tune the nominal PID [15] and two degree of freedom based PID [16] controller parameters for containing system frequency for a distributed microgrid system with different components such as wind, solar thermal, diesel, ultracapacitor (UC). Some studies are by leveraging different techniques such as firefly (FF), cuckoo search (CS) techniques based classical PID controllers. Successful implementation details and result analyses are presented in [17,18]. A research carried for frequency stabilization of hybrid power system incorporate with wind, fuel cell, battery, Aqua Electrolyze (AE), diesel generator (DG), and UC with the help of a cascade PD-PID controller [19]. Wind and super conducting magnetic energy systems are incorporated with non-renewable sources like diesel power plants to study and analyse the frequency regulation of hybrid power system using a PID controller. In this research, a controller's gain values are tuned by utilizing mine blast technique (MBA) [20].

In addition to the PID controller, fractional order PID (FOPID) controller is also used to control frequency in microgrids. Multi-objective extremal optimization (MOEO) is used to make effective FOPID based frequency controller design for minimizing frequency deviation and controller output signal simultaneously [21]. In [22], it is aimed the use of FOPID controller for absorbing the system frequency deviation in stochastic and nonlinear model

of a microgrid. Kriging based surrogate modeling is used not only for tuning the controller parameters, but also for reducing the time taken for optimization [22]. In [23], cascade fractional-order controller that consists of three degrees of freedom proportional-integral derivative controllers was proposed. While the objective is to control the system frequency in a much better way, these techniques lead to demerits like higher-order controller design, complexity in implementations, and prove unsuitable for all operating conditions.

Hence, to overcome these difficulties, artificial intelligence (AI) techniques like fuzzy logic control (FLC) [24,25] were proposed to minimize the frequency deviation in distributed microgrid power systems. Again, these methods suffer from demerits like the extensive preliminary knowledge required for selecting the FLC parameters and greater computational need in the analysis. An alternative way of solving the issues is to use an effective evolutionary algorithmic technique like population based sine-cosine technique (SCA) due to of their simplicity in implementation and robust approach [26]. Also, they require relatively fewer control parameters to be tuned to provide better convergence characteristics and to achieve improved stability. In order to enhance the dynamic responses effectively with fewer control parameters, in this paper, a maiden two-stage integral-proportional-derivative with one plus integral (IPD-(1+I)) controller structure has been developed for the first time. Owing to the advantage the proposed control stratagem, this paper proposed the SCA technique to select the gains of the novel (IPD-(1+I)) controller so that the frequency deviations will be minimized and the frequency stability will be enhanced under different operating conditions. In addition to the graphical analysis, the proposed controllers' performance is tested by calculating different decision parameters such as settling time, peak overshoot, and undershoot. The detailed contributions of the paper are discussed as follows.

- (a) Design and implementation of a (IPD-(1+I)) controller and development of it's transfer function for a multi-source islanded micro grid system's (MS-I μ GS) frequency response model.
- (b) Performing different simulation case studies to test the dynamic performance of the proposed control stratagem and analysed the results for frequency deviation and power sharing characteristics of other subsystems. The performance of the study is reported via the measurement of performance indices (J), J_{FOD}, settling time, undershoot, and overshoot.
- (c) The performance of the proposed stratagem is validated using real-time wind data.

This paper is structured as follows. The mathematical modeling of a sustainable microgrid system is presented in Section 2. This is followed by a description of the proposed controller and optimization technique in Sections 3 and 4. The acquired simulation results from the proposed model are presented in Section 5, followed by the conclusions in Section 6.

2. Details of the Proposed Frequency Response Model

In this research, a microgrid is developed in MATLAB Simulink environment. The renewable sources are wind, parabolic trough solar thermal, bio-diesel generation and energy storing system based on solid-oxide fuel cell (SOFC) technology. The schematic view and detailed mathematical model without considering non-linearities and converter actions of the proposed sustainable microgrid are shown in Figure 1. The considered wind data and SCA technique's parameters are reported in the Appendix A. This section presents the main components and their corresponding mathematical representation for the selected microgrid case study.

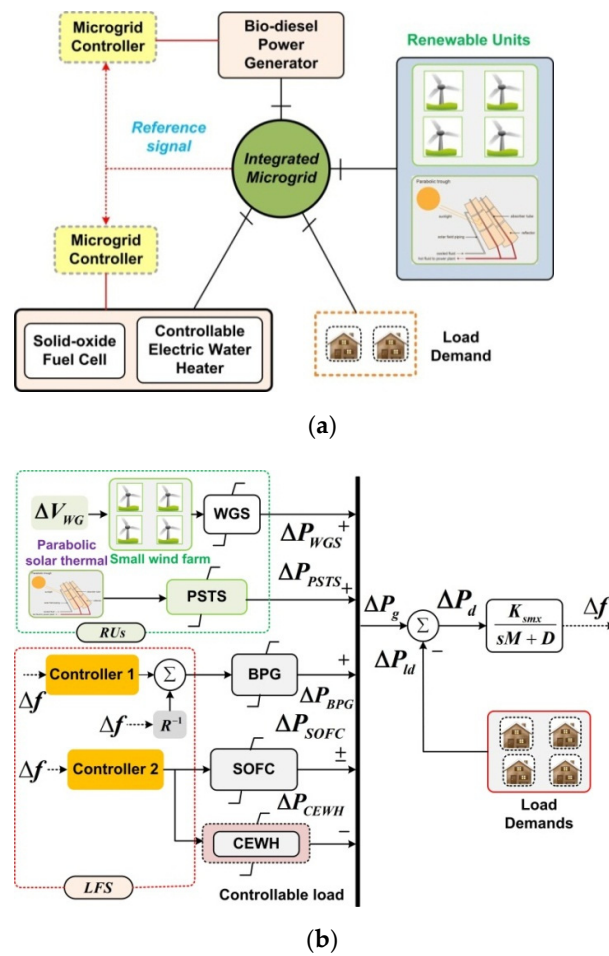


Figure 1. (a) Schematic of the proposed MS-IμGS, (b) The overall structure and system modeling of the studied MS-IμGS.

2.1. Dynamic Modeling of Generation Units

2.1.1. Wind Generation System (WGS)

The intermittent nature wind driven power is produced by wind turbine through mechanical to electrical power conversion. That extractable wind power is very much dependent on wind velocity and other inherent identifications of the wind turbine. The first stage mechanical power (P_{WG}) from wind velocity can be expressed as [27];

$$P_{WG} = 0.5\rho \cdot V_{WG}^3 \cdot S_b \cdot C_p(\lambda, \beta) \tag{1}$$

Taking into account that ρ , V_{WG} , S_b , and C_p are the air density (kg/m^3), intermittent wind velocity (m/s), turbine’s blade swept area (m^2), and the extractable power co-efficient, respectively, the expression of C_p could be illustrated as;

$$10C_p = 5.17 \left(\frac{1160}{\lambda + 0.08\beta} - \frac{40.6}{1 + \beta} - 0.8\beta - 50 \right) e^{(-\frac{21}{\lambda})} + 0.068\lambda \tag{2}$$

The internal function λ and β are the tip-speed ratio and blade pitch angle respectively. A real-time recorded datasheet (provided by National Institute of Wind Energy, India) of Akkanayakanpatti wind power station is considered in this work, as shown in the

Appendix A. The rate of change of considered station’s wind power generation (ΔP_{WGS}) with its complete transfer function model could be represented as below [28]:

$$P_{WGS} = \begin{cases} 0, & V_{WG} < V_{cut-in} \text{ || } V_{WG} > V_{cut-out} \\ P_{rated}, & V_{rated} \leq V_{WG} \leq V_{cut-out} \\ (0.001312 V_{WG}^6 - 0.04603 V_{WG}^5 + 0.3314 V_{WG}^4 \\ + 3.687 V_{WG}^3 - 51.1 V_{WG}^2 + 2.33 V_{WG} + 366), & else \end{cases} \quad (3)$$

$$\Delta P_{WGS} = \begin{cases} 0, & V_{WG} < V_{cut-in} \text{ || } V_{WG} > V_{cut-out} \\ 0, & V_{rated} \leq V_{WG} \leq V_{cut-out} \\ ([0.007872 V_{WG}^5 - 0.23015 V_{WG}^4 + 1.3256 V_{WG}^3 \\ + 11.061 V_{WG}^2 - 102.2 V_{WG} + 2.33] \cdot \Delta V_{WG}), & else \end{cases} \quad (4)$$

$$G_{WGSx}(s) = K_{WGSx} \cdot \left(\frac{1}{sT_{WGSx} + 1} \right)$$

where V_{cut-in} and $V_{cut-out}$ are the cut-in and cut-out wind velocities in m/s. K_{WGSx} and T_{WGSx} are the gain and constant time of wind generation system.

2.1.2. Parabolic Trough Solar Thermal System (PSTS)

The PSTS power conversation system comprising of solar beam, oil filled solar collector, governor-turbine which helps to produce electrical energy. This solar thermal system has differentiate from other solar thermal system due it’s low investment cost with higher operational efficiency and more concentrate solar radiation on the receiver channel. Different kind of thermal storages can use in PSTS. As explained in [29], the thermal storages can be neglected. The parabolic trough collector’s efficiency could be illustrated as;

$$\eta_{Cx} = K[73.8 - (0.006460 \cdot \Delta T)] - \left[(12.16 \cdot \Delta T) / I_D - 0.0641 \cdot (\Delta T)^2 / I_D \right] \quad (5)$$

where

$$K = \cos \alpha - 0.0003512\alpha - 0.00003137\alpha^2 \quad (6)$$

The actual temperature ($^{\circ}C$) of PSTS is formed as ΔT . I_D ($= 873 \text{ W/m}^2$) is the direct solar irradiance. The incident angle is termed as K . From Equation (5), the change in parabolic trough collector efficiency could be formed as:

$$\Delta \eta_{PC} = \Delta I_D \cdot \left\{ \frac{1}{I_D^2 \cdot (12.16 \cdot \Delta T + 0.0641 \cdot (\Delta T)^2)} \right\} \quad (7)$$

$$P_{PSTS} = \eta_{ox} \cdot P_{inp} \quad (8)$$

The overall efficiency η_{ox} can be expressed as;

$$\eta_{ox} = \eta_{Cx} \cdot \eta_{Gx} \cdot \eta_{Tx} \quad (9)$$

The net change in PSTS power (ΔP_{PSTS}) could be expressed as:

$$\Delta P_{PSTS} = (\Delta \eta_{Cx} \cdot \Delta \eta_{Gx} \cdot \Delta \eta_{Tx}) \cdot P_{inp} \quad (10)$$

The transfer function of the solar thermal power plant collector G_{Cx} , governor G_{Gx} , and the turbine G_{Tx} are modeled as following:

$$G_{Cx}(s) = K_{Cx} \left(\frac{1}{sT_{Cx} + 1} \right) \quad (11)$$

$$G_{Gx}(s) = K_{Gx} \left(\frac{1}{sT_{Gx} + 1} \right) \quad (12)$$

$$G_{Tx}(s) = K_{Tx} \left(\frac{1}{sT_{Tx} + 1} \right) \quad (13)$$

where K_{Cx} , K_{Gx} , and K_{Tx} are the gains of collector, governor and turbine. The constant time values of the same parameters are symbolized by T_{Cx} , T_{Gx} , and T_{Tx} . With a gain value of 1, the constant time value of power converter is assumed by 0.01 s.

2.1.3. Bio-Diesel Power Generation (BPG)

The projected biodegradable BPG unit is utilized in this research work encloses islanded microgrid system for higher efficient based minimal carbon emitted backup power generation. It's independently proficient of delivering the deficiency of power and could be minimize the power mismatch between generation and demand. The linearized model of BPG could be formed as [30]:

$$\Delta W_{BPG} = W(s) - (R^{-1} \cdot \Delta f) \quad (14)$$

$$\Delta P_{BPG} = \Delta P_{GCE} \cdot \left(\frac{K_{CEx}}{T_{CEx}s + 1} \right) \quad (15)$$

where ΔW_{BPG} and $W(s)$ are the change in input error of BPG and the output control signal of the controller. The droop constant is represented by R (Hz/p.u. MW). K_{CEx} and T_{CEx} are the gain and constant time delay of BPG.

2.1.4. Solid-Oxide Fuel Cell (SOFC)

The solid-oxide fuel cell act as an important component due to its higher temperature (600–1000 °C), efficiency (~80%) with lower polluted gas emission. The SOFC power generation system is higher order system, however due to small signal analysis, the linearized first order transfer function is taken as depicted in Equation (16) [31].

$$G_{SOFCx}(s) = \frac{K_{SOFCx}}{sT_{SOFCx} + 1} \quad (16)$$

where the gain and constant time values of SOFC is represented by K_{SOFCx} and T_{SOFCx} .

2.2. Dynamic Modeling of Controllable Electric Water Heater

Besides the different generations units to take care of load demands for optimal frequency stabilization a controllable electric water heater (CEWH) is considered in the proposed model. The first order CEWH model is adopted here as follows:

$$G_{CEWHx}(s) = \frac{K_{CEWHx}}{T_{CEWHx}s + 1} \quad (17)$$

where the gain and constant time values of CEWH is represented by K_{CEWHx} and T_{CEWHx} .

2.3. Dynamic Modeling of Power System and Load

Considering all the system components, the first order sustainable microgrid power system’s transfer function, $G_{smx}(s)$, could be modeled as [30]:

$$G_{smx}(s) = \frac{K_{smx}}{sM_{smx} + D_{smx}} \tag{18}$$

K_{smx} , M_{smx} and D_{smx} are the gain, inertia value (s) and damping co-factor (p.u./Hz) of the hybrid microgrid system.

Here, the targeted Δf can be formulated as [30]:

$$\Delta f = \left(\frac{K_{smx}}{sM + D} \right) \cdot \Delta P_g \tag{19}$$

$$\Delta P_g = \left(\begin{array}{c} \Delta P_{RUs} + \Delta P_{BPG} \\ \pm \Delta P_{SOFC} - \Delta P_{CEWH} \end{array} \right) = \Delta P_{ld} \rightarrow 0 \tag{20}$$

$$\Delta P_d = \Delta P_g - \Delta P_{ld} \tag{21}$$

The specified values of the system parameters are displayed in Table 1.

Table 1. Utilized parameters and abbreviations.

Symbol	Nomenclature	Value
ΔP_{ld}	Net load demand of MS-I μ GS	-
Δf	frequency deviation (Hz) of MS-I μ GS	-
ΔP_g	Net generated power of MS-I μ GS	-
D	Microgrid damping co-efficient	0.1
M	Microgrid inertia constant	0.12
K_{CEx}	Gain of engine delay of BPG	1
T_{CEx}	Constant time engine delay of BPG	0.4 s
K_{WGSx}	Gain of wind	1
T_{WGSx}	Time constant wind	5 s
K_{Cx}, K_{Gx}, K_{Tx}	Gain of collector, governor and turbine of PSTS	1.8, 1, 1
T_{Cx}, T_{Gx}, T_{Tx}	Constant time of collector, governor and turbine of PSTS	1.8 s, 1 s, 3 s
K_{SOFCx}	Gain of SOFC	1
T_{SOFCx}	Time constant of SOFC	0.2 s
K_{CEWHx}	Gain of CEWH	1
T_{CEWHx}	Time constant of CEWH	0.1 s
t_{sim}	Simulated run time of MS-I μ GS	100 s

3. Designed of Two-Stage (IPD-(1+I)) Controller Model

In frequency stabilization problem analysis, the optimal adjustment of the controller is interrelated. So, the associated the load frequency controller are tuned based on a certain algorithm. To meet higher stability, a robust control method is needed. Using only droop method is insufficient for advanced control purposes. Thus, the secondary control loop is needed for better control of the frequency fluctuation of the distributed power network. The nominal proportional-integral-derivative (PID) controller has been used in many industrial and power system applications. At the moment, to meet the challenges of frequency regulation in a reliable and flexible manner, two-stage controllers are at the forefront of analytical trends. That’s due to their robustness and better adjustment of controller parameters than classical PID controllers. The general stratagem of proposed two stage

integral-proportional-derivative with one plus integral (IPD-(1+I)) controller is depicted in Figure 2. The control is performed using the input change in frequency deviation signal. The formulation of (IPD-(1+I)) controller with its transfer function modeling could be expressed as:

$$U_c(s) = \Delta f \cdot \{IPD(1 + I)\} \tag{22}$$

$$G_{\{IPD-(1+I)\}}(s) = \left(\frac{K_{Ii}}{s} + K_P + K_D s \right) \left(1 + \frac{K_{Ii}}{s} \right); \text{ i.e.; } i = (1, 2 \dots) \tag{23}$$

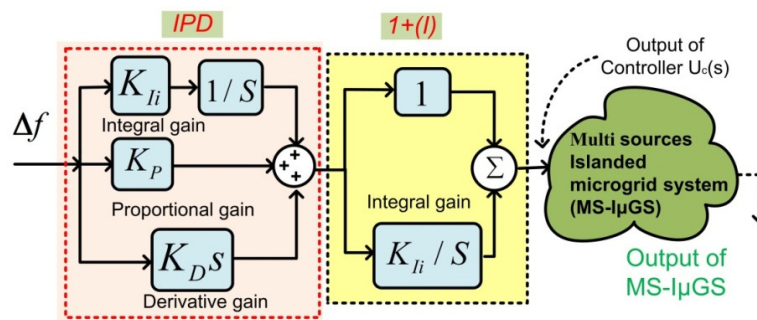


Figure 2. Structural framework of the proposed two-stage (IPD-(1+I)) controller.

From the structure shown in Figure 2, the operation is executed over two stages, where four control parameters are considered. In this anatomy, the advantages of the proposed (IPD-(1+I)) controller are the enhancement of system stability by reducing the peak deviation and transient response improvement. This is important because the PID controller is not as effective under transient operation. These constant parameters play a crucial role in stabilizing the system response. Hence, to get the optimum value of the proposed controller, different optimization techniques are applied.

4. Detail of Sine-Cosine Algorithmic Technique (SCA)

It has been reported that sine and cosine functions provide several random solutions for the optimal result using SCA technique [26]. This technique adaptively maintains the exploration and exploitation phases to get local as well as global optimal results. The ‘N’ numbers of search variables are examined in every iteration and provide the optimal result through fitness values. Every search variable is signified ‘d’ dimensional decision vector $Q_i = (q_{i1}, q_{i2}, \dots, q_{id})$. Following this manner, the best position S is attained for the total search variables at every iteration. SCA technique is designed considering position updating for two phases as in (24) and (25) [26].

$$Q_i^{t+1} = \left\{ \begin{array}{l} Q_i^t + R_1 \cdot \sin(R_2) \cdot |R_3 \cdot S_i^t - Q_i^t|; \text{ if } R_4 < 0.5 \\ Q_i^t + R_1 \cdot \cos(R_2) \cdot |R_3 \cdot S_i^t - Q_i^t|; \text{ if } R_4 \geq 0.5 \end{array} \right\} \tag{24}$$

where Q_i^t, S_i^t are the position of present solution and targeted position of i th dimension at t^{th} iterations, respectively. The R_1, R_2, R_3, R_4 are key random numbers, where R_1 indicates the movement region. This movement can be inside or outside of the search space. R_2 defines the location movement towards or outwards of the targeted solution. R_3 is the randomized weight factor for targeted destination and its emphasis, where $R_3 < 1$ indicated emphasis whereas $R_3 > 1$ indicates otherwise. In addition, R_4 equally selects sine and cosine components. The inside/outside updated positions can be done by relocating the sine-cosine mathematical functions as illustrated in [26]. To get global optima, alteration in R_1 is done to balance exploration–exploitation by leveraging (25).

$$R_1 = \left\{ b - I \cdot \left(\frac{b}{T} \right) \right\} \tag{25}$$

where $b =$ algorithmic constant, I is present iteration, and $T =$ maximum iterations. The detailed steps of SCA technique is demonstrated as flowchart in Figure 3a. The Simulink model in Figure 1b is invoked by this SCA algorithm to assess/update the values in each iteration by passing the tuned controller gains within their boundary limits. The detailed simulation results and performance comparisons are discussed in the following section. The detail parameters of the SCA techniques are shown in Appendix A.

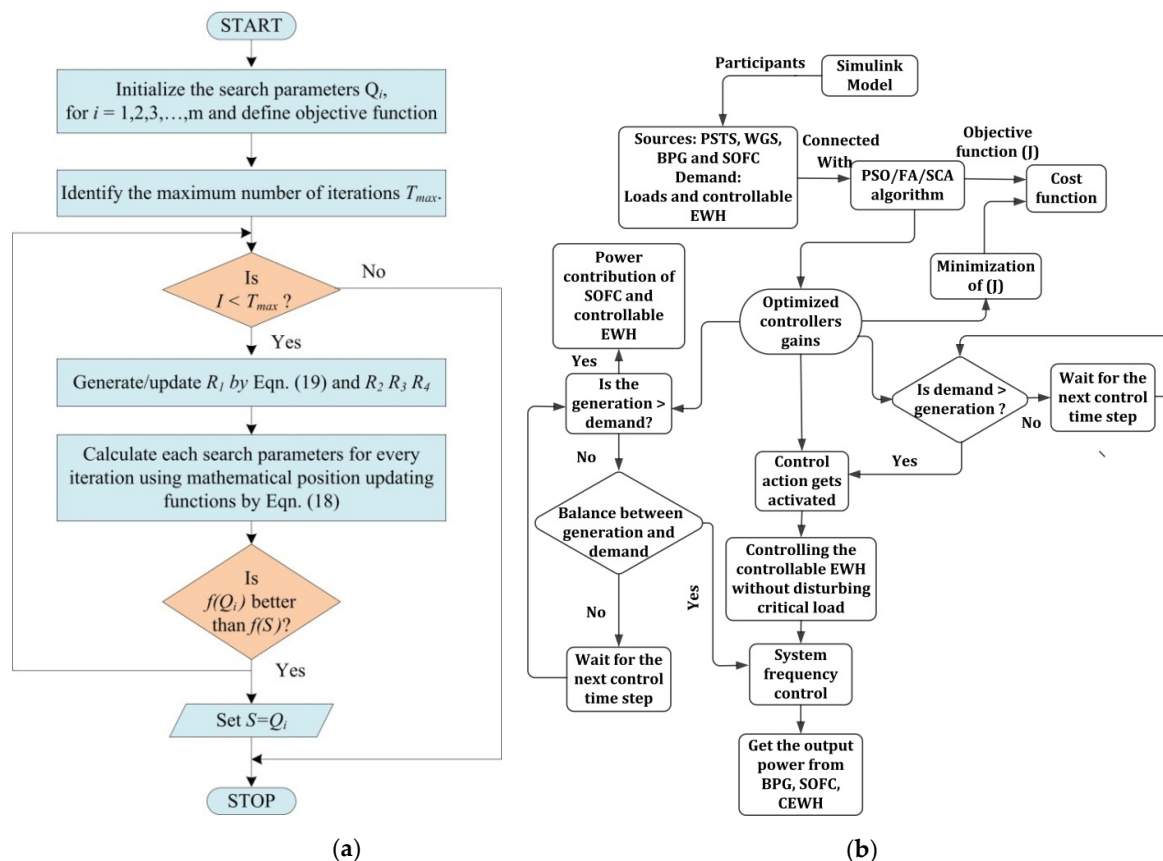


Figure 3. (a) Flow diagram for implementing the sine-cosine technique, (b) Overall control stratagem for the proposed frequency response hybrid microgrid model.

On the other hand, the main aim of these abovementioned algorithms is to minimize the objective function, i.e., integral square error (ISE) as denoted as J , presented in (26), which has been optimized by considered three different algorithms.

$$J = \int_0^{t_{sim}} \{(\Delta f)^2 \cdot dt\} \tag{26}$$

where Δf is the frequency change for the simulated response time (t_{sim}). In order to visualize the overall control strategy a flow diagram has been depicted as shown in Figure 3b. As the proposed (IPD-(1+I)) controller is used in this study, hence the controller must have constraints such as:

$$\begin{aligned} K_{I1 \min} &\leq K_{I1} \leq K_{I1 \max} \\ K_{P \min} &\leq K_P \leq K_{P \max} \\ K_{D \min} &\leq K_D \leq K_{D \max} \\ K_{I2 \min} &\leq K_{I2} \leq K_{I2 \max} \end{aligned} \tag{27}$$

where $I = (1, 2, \dots)$.

5. Simulation Results and System Validation

This section is devoted to demonstrating the dynamic performance of the proposed control stratagem for multi-source islanded microgrid system (MS-I μ GS). The simulations are performed on MATLAB[®] Simulink[®] R2015a software platform. In the proposed system, the dynamic responses are tested with the employment of traditional PI, PID and novel (IPD-(1+I)) controllers. To optimize gain parameters, different optimization algorithms have been leveraged. The system's dynamic performance has been analyzed with different parameters, such as peak oscillations and settling time, significantly using optimization techniques tuned controllers. The following subsections present the result analysis by taking the different case studies. Finally, the real-time validation is done by considering real-recorded natural wind velocity data where the dynamic response have also been analyzed. The main parameters of the studied microgrid power systems are tabulated in Table 1.

5.1. Case 1: Frequency Response Study under Non-Accessibility of All RUs

In this sub-section, the frequency fluctuation and other sub-systems power sharing are studied by considering traditional PI, PID and novel (IPD-(1+I)) controllers for non-accessibility of all RUs. As far as load perturbation is concerned, it is consumed by 30% at $t = 0$ s onwards and the corresponding frequency and power sharing of other sub-networks are observed using SCA optimized traditional PI, PID, and (IPD-(1+I)) controllers. The frequency deviation profile of the MS-I μ GS in the presence of different controller's is shown in Figure 4a. Whereas the corresponding comparative power sharing's of different components are displayed in Figure 4b–d. The tuned numerical values of considered controllers are depicted in Table 2. The designed controllers using SCA technique shows its ability to damp the transient frequency oscillation compared to the other considered traditional controllers as depicted in Figure 4a. It is also found that, by adopting SCA: (IPD-(1+I)) stratagem, the frequency stabilization responses are enhanced with lower settling time (ST) compared to the other SCA:PI SCA:PID stratagems, as summarized in Table 2, wherein the comparative maximum overshoot (+MXO), maximum undershoot(−MXU), and the settling time (ST) are measured. Moreover, this distinguished performance of the proposed (IPD-(1+I)) controller is validated by showing the convergence curve (J) as displayed in Figure 4e. The FOD based performance index (J_{FOD}) of the isolated system as expressed in (28) are estimated for all controllers and compared in Table 2.

$$J_{FOD} = \left\{ (+MXO)^2 + (-MXU)^2 + (ST)^2 \right\} \quad (28)$$

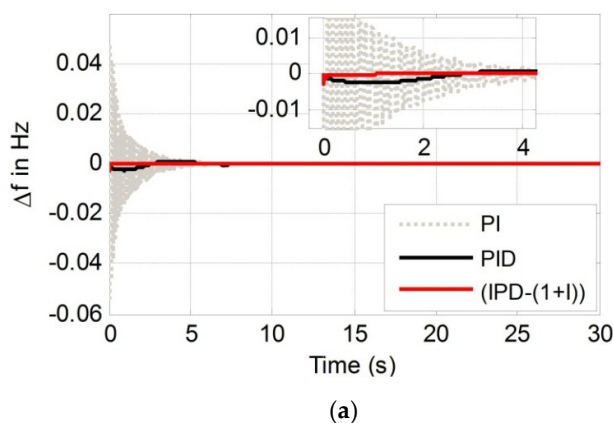


Figure 4. Cont.

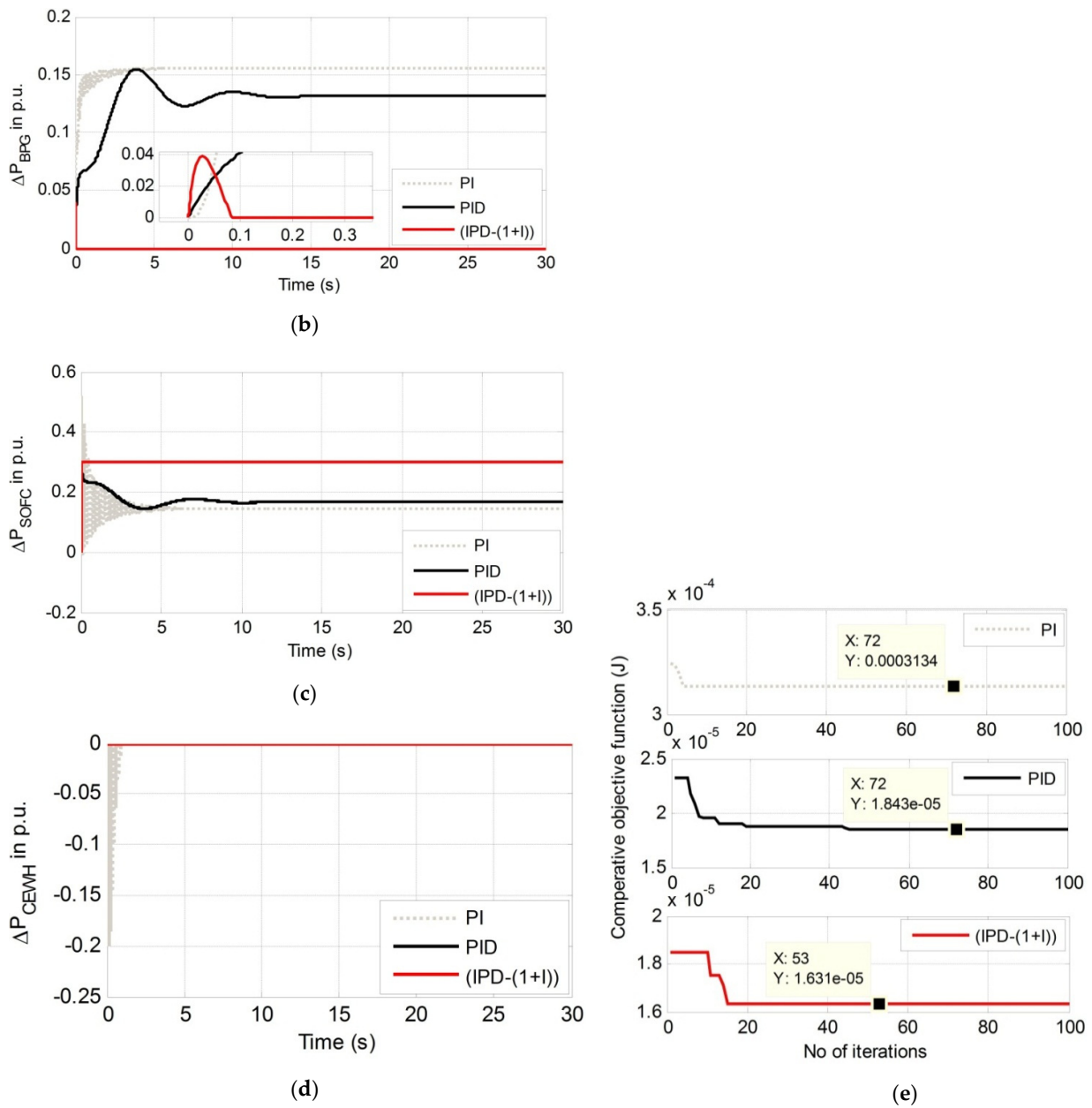


Figure 4. Comparison of the dynamic response of PI, PID with the proposed (IPD-(1+I)) controller (a) frequency deviation, (b) power output of BPG, (c) power output of SOFC, (d) power output of CEWH and (e) objective functions (J).

Table 2. Controllers' gains with comparative performance parameters under 100 iterations.

Controllers		PI	PID	(IPD-(1+I))
Maximum Overshoot (+MXO)				
Δf (in Hz)		0.0551	0.0008	0.00003
Maximum Undershoot (-MXU)				
Δf (in Hz)		0.0480	0.0025	0.0023
Settling time (T_{ST})				
Δf (in s)		5.468	4.075	1.825
Minimum value of J (J_{min})				
		3.13×10^{-4}	1.84×10^{-5}	1.63×10^{-5}
Figure of demerits (J_{FOD})				
		29.904	16.605	3.330
Optimized controllers' values				
Controller-1	K_{P1}	39.60	0.00091	39.48
	K_{I11}	32.46	39.06	46.67
	K_{D1}	-	22.02	39.92
	K_{I12}	-	-	14.27
Controller-2	K_{P2}	49.58	49.97	4.28
	K_{I21}	30.18	48.75	14.40
	K_{D2}	-	49.08	15.81
	K_{I22}	-	-	40.34

5.2. Case 2: Frequency Response Study under Concurrent Random Change in RU's Generation and Load

This section deals the optimal tuning of controller gain values using considered optimization techniques such as PSO, FA, and SCA. The extent of the robustness of the designed controller based techniques is examined under the state of real-recorded random wind weather data and other collective disturbances. The varying random input illustrated in Figure 5a. The system's corresponding frequency deviation is demonstrated in Figure 5b and the other subsystem power sharing contribution is depicted in Figure 5c,d. The tuned numerical values under considered optimization techniques tuned designed controllers are depicted in Table 3. It can be ascertained from Figure 5b–d that the change in frequency and other subunits performs better under SCA tended novel two-stage controller. Whereas, the designed controllers using the individual PSO and FA suffer from prolonged damped oscillations as shown in Figure 5b–d. Further exploration under random weather condition illustrates the competency of the proposed stratagem. Also, this case study demonstrates the suggested algorithm's efficacy with the proposed controller.

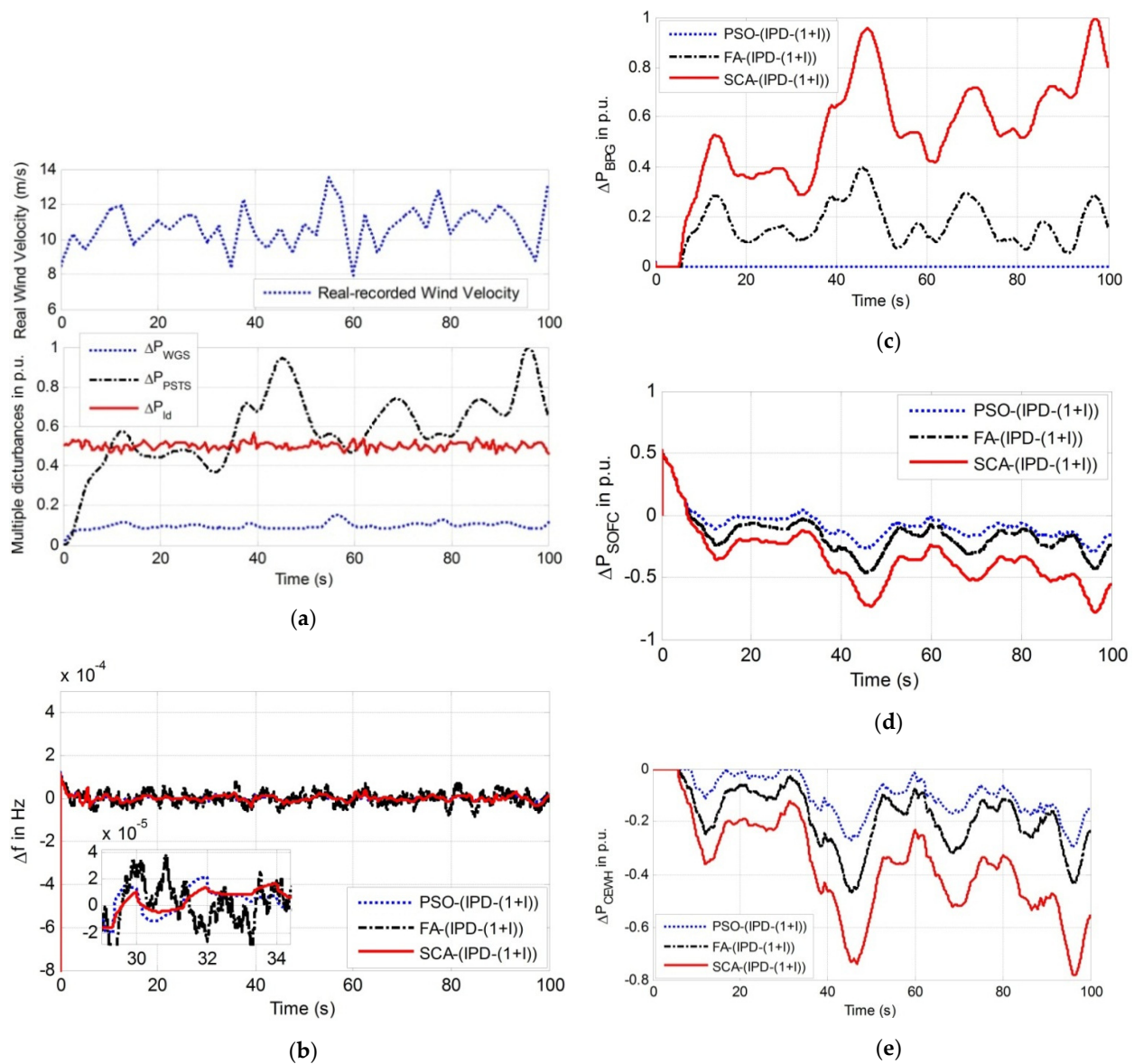


Figure 5. Comparison of the dynamic response when (IPD-(1+I)) controller is optimized with PSO, FA with SCA (a) Real-time data based multiple random disturbances (b) frequency deviation, (c) power output of BPG, (d) power output of SOFC, and (e) power output of CEWH.

Table 3. (IPD-(1+I)) controller’s parameters for the selected case study (Case 2).

Techniques		PSO	FA	SCA
Optimized Controllers’ Values				
Controller-1	K_{P1}	48.12	24.45	49.87
	K_{I11}	18.46	40.41	49.99
	K_{D1}	20.89	18.28	18.30
	K_{I12}	44.86	39.60	42.48
Controller-2	K_{P2}	49.87	35.95	47.77
	K_{I21}	39.11	39.86	37.76
	K_{D2}	20.05	25.32	21.59
	K_{I22}	49.53	49.89	49.96

6. Conclusions

In this paper, a novel control stratagem is developed by optimizing a novel two-stage (IPD-(1+I)) controller structure with a recently developed sine-cosine technique (SCA) for the frequency regulation of MS-I μ GS. The combination of renewable power sources such as wind, parabolic-trough solar thermal, bio-diesel units in addition to solid-oxide fuel cell and controllable electric water heater is studied. As a novelty, the development of the (IPD-(1+I)) controller is applied for a frequency response model through the SCA technique and the performances are presented and compared with other traditional controllers. Moreover, the system's dynamic responses are compared through various performance indices, such as settling time, overshoot, undershoot, ISE error function (J), and estimated J_{FOD} index values. The analysis of the comparative J values shows the percentage improvement of J_{min} with proposed (IPD-(1+I)) controller compared to traditional PI and PID are 94.79% and 11.41% respectively. As an after stage, the SCA technique has been applied and compared with other technique, such as PSO and FA. Further, real-recorded wind data have been considered for the real-time validation of the proposed control stratagem. It was observed that the SCA-(IPD-(1+I)) controller can manage system disturbances and enable the required power sharing between sub-systems. Performance tests validate its suitability for use in microgrids with high renewable energy penetration. Root locus analysis could be conducted in the future to judge the stability of the MS-I μ GS.

Author Contributions: Conceptualization, A.L., S.M.S.H., D.C.D. and T.S.U.; methodology, A.L. and S.M.S.H.; software, A.L.; validation, A.L.; formal analysis, A.L., S.M.S.H., D.C.D. and T.S.U.; investigation, A.L.; data curation, A.L. and D.C.D.; writing—original draft preparation, A.L.; writing—review and editing, S.M.S.H., D.C.D. and T.S.U.; visualization, A.L., S.M.S.H. and D.C.D.; project administration, S.M.S.H. and T.S.U.; funding acquisition, S.M.S.H. All authors have read and agreed to the published version of the manuscript.

Funding: This research received no external funding.

Conflicts of Interest: The authors declare no conflict of interest.

Appendix A

WGS: Recorded date: 1 July 2016, Min^m flow of wind: 7.4804 (m/s); Max^m flow of wind: 14.08 m/s; Average flow of wind: 10.922 m/s; SD: 1.1895.

SCA parameters: $b = 2$, No search parameters = 20, Max^m iterations = 100, $R_4 = [0, 1]$.

References

1. Almeshqab, F.; Ustun, T.S. Lessons learned from rural electrification initiatives in developing countries: Insights for technical, social, financial and public policy aspects. *Renew. Sustain. Energy Rev.* **2019**, *102*, 35–53. [CrossRef]
2. The Sustainable Development Goals Report 2019. United Nations 2019. Available online: <https://unstats.un.org/sdgs/report/2019/The-Sustainable-Development-Goals-Report-2019.pdf> (accessed on 11 April 2021).
3. Tabak, A.; Özkaymak, M.; Tahir, M.; Oktay, H. Optimization and Evaluation of Hybrid PV/WT/BM System in Different Initial Costs and LPSP Conditions. *Int. J. Adv. Comput. Sci. Appl.* **2017**, *8*, 123–131. [CrossRef]
4. Boukelia, T.; Mecibah, M. Parabolic trough solar thermal power plant: Potential, and projects development in Algeria. *Renew. Sustain. Energy Rev.* **2013**, *2*, 288–297. [CrossRef]
5. Rakhshani, E.; Remon, D.; Cantarellas, A.M.; Rodriguez, P. Analysis of derivative control based virtual inertia in multi-area high-voltage direct current interconnected power systems. *IET Gener. Transm. Distrib.* **2016**, *10*, 1458–1469. [CrossRef]
6. Ustun, T.S.; Aoto, Y. Analysis of Smart Inverter's Impact on the Distribution Network Operation. *IEEE Access* **2019**, *7*, 9790–9804. [CrossRef]
7. Latif, A.; Hussain, S.M.S.; Das, D.C.; Ustun, T.S. State-of-the-art of controllers and soft computing techniques for regulated load frequency management of single/multiarea traditional and renewable energy based power systems. *Appl. Energy* **2020**, *266*, 114858. [CrossRef]
8. Hosseinzadeh, M.; Salmasi, F.R. Robust Optimal Power Management System for a Hybrid AC/DC Micro-Grid. *IEEE Trans. Sustain. Energy* **2015**, *6*, 675–687. [CrossRef]
9. Schonbergerschonberger, J.; Duke, R.; Round, S.D. DC-Bus Signaling: A Distributed Control Strategy for a Hybrid Renewable Nanogrid. *IEEE Trans. Ind. Electron.* **2006**, *53*, 1453–1460. [CrossRef]

10. Jiayi, H.; Chuanwen, J.; Rong, X. A review on distributed energy resources and MicroGrid. *Renew. Sustain. Energy Rev.* **2008**, *12*, 2472–2483. [[CrossRef](#)]
11. Alhelou, H.H.; Hamedani-Golshan, M.E.; Zamani, R.; Heydarian-Forushani, E.; Siano, P. Challenges and opportunities of load frequency control in conventional, modern and future smart power systems: A comprehensive review. *Energies* **2018**, *11*, 2497. [[CrossRef](#)]
12. Das, D.C.; Roy, A.K.; Sinha, N. GA based frequency controller for solar thermal–diesel–wind hybrid energy generation/energy storage system. *Int. J. Electr. Power Energy Syst.* **2012**, *43*, 262–279. [[CrossRef](#)]
13. Rout, U.K.; Sahu, R.K.; Panda, S. Design and analysis of differential evolution algorithm based automatic generation control for interconnected power system. *Ain Shams Eng. J.* **2013**, *4*, 409–421. [[CrossRef](#)]
14. Dash, P.; Saikia, L.C.; Sinha, N. Flower Pollination Algorithm Optimized PI-PD Cascade Controller in Automatic Generation Control of a Multi-area Power System. *Int. J. Electr. Power Energy Syst.* **2016**, *82*, 19–28. [[CrossRef](#)]
15. Hussain, I.; Ranjan, S.; Das, D.C.; Sinha, N. Performance analysis of flower pollination algorithm optimized PID controller for wind-PV-SMES-BESS-diesel autonomous hybrid power system. *Int. J. Renew. Energy Res.* **2017**, *7*, 643–651.
16. Hussain, I.; Das, D.C.; Sinha, N.; Latif, A.; Hussain, S.M.S.; Ustun, T.S. Performance Assessment of an Islanded Hybrid Power System with Different Storage Combinations Using an FPA-Tuned Two-Degree-of-Freedom (2DOF) Controller. *Energies* **2020**, *13*, 5610. [[CrossRef](#)]
17. Latif, A.; Das, D.C.; Ranjan, S.; Hussain, I. Integrated demand side management and generation control for frequency control of a microgrid using PSO and FA based controller. *Int. J. Renew. Energy Res.* **2018**, *8*, 188–199.
18. Latif, A.; Pramanik, A.; Das, D.C.; Hussain, I.; Ranjan, S. Plug in hybrid vehicle-wind-diesel autonomous hybrid power system: Frequency control using FA and CSA optimized controller. *Int. J. Syst. Assur. Eng. Manag.* **2018**, *9*, 1147–1158. [[CrossRef](#)]
19. Gorripotu, T.S.; Ramana, P.; Sahu, R.K.; Panda, S. Sine Cosine Optimization Based Proportional Derivative-Proportional Integral Derivative Controller for Frequency Control of Hybrid Power System. In *Computational Intelligence in Data Mining*; Springer: Singapore, 2020; pp. 789–797.
20. Alattar, A.H.; Selem, S.I.; Metwally, H.; Ibrahim, A.; Aboelsaud, R.; Tolba, M.A.; El-Rifaie, A.M. Performance enhancement of micro grid system with SMES storage system based on mine blast optimization algorithm. *Energies* **2019**, *12*, 3110. [[CrossRef](#)]
21. Wang, H.; Zeng, G.; Dai, Y.; Bi, D.; Sun, J.; Xie, X. Design of a fractional order frequency PID controller for an islanded microgrid: A multi-objective extremal optimization method. *Energies* **2017**, *10*, 1052. [[CrossRef](#)]
22. Pan, I.; Das, S. Kriging based surrogate modeling for fractional order control of microgrids. *IEEE Trans. Smart Grid.* **2015**, *6*, 36–44. [[CrossRef](#)]
23. Guha, D.; Roy, P.K.; Banerjee, S. Equilibrium optimizer-tuned cascade fractional-order 3DOF-PID controller in load frequency control of power system having renewable energy resource integrated. *Int. Trans. Electr. Energy Syst.* **2021**, *31*, e12702. [[CrossRef](#)]
24. Karimipouya, A.; Abdi, H. Microgrid frequency control using the virtual inertia and ANFIS-based Controller. *Int. J. Ind. Electron. Control Optim.* **2019**, *2*, 145–154.
25. Lal, D.K.; Barisal, A.K.; Tripathy, M. Load frequency control of multi area interconnected microgrid power system using grasshopper optimization algorithm optimized fuzzy PID controller. In Proceedings of the 2018 Recent Advances on Engineering, Technology and Computational Sciences (RAETCS), Allahabad, India, 6–8 February 2018; pp. 1–6.
26. Mirjalili, S. SCA: A sine cosine algorithm for solving optimization problems. *Knowl. Based Syst.* **2016**, *96*, 120–133. [[CrossRef](#)]
27. Shang-Guan, X.; He, Y.; Zhang, C.; Jiang, L.; Spencer, J.W.; Wu, M. Sampled-data based discrete and fast load frequency control for power systems with wind power. *Appl. Energy* **2020**, *259*, 114202. [[CrossRef](#)]
28. Khooban, M.H.; Dragicevic, T.; Blaabjerg, F.; Delimar, M. Shipboard microgrids: A novel approach to load frequency control. *IEEE Trans. Sustain. Energy* **2018**, *9*, 843–852. [[CrossRef](#)]
29. Kuravi, S.; Trahan, J.; Goswami, D.Y. Thermal energy storage technologies and systems for concentrating solar power plants. *Prog. Energy Combust. Sci.* **2013**, *39*, 285–319. [[CrossRef](#)]
30. Latif, A.; Hussain, S.M.S.; Das, D.C.; Ustun, T.S. Double stage controller optimization for load frequency stabilization in hybrid wind-ocean wave energy based maritime microgrid system. *Appl. Energy* **2021**, *282*, 116171. [[CrossRef](#)]
31. Taghizadeh, M.; Hoseintabar, M.; Faiz, J. Frequency control of isolated WT/PV/SOFC/UC network with new control strategy for improving SOFC dynamic response. *Int. Trans. Electr. Energy Syst.* **2015**, *25*, 1748–1770. [[CrossRef](#)]